

Regioselective Catenation of Dinuclear Palladium and Platinum Metallo-cycles Promoted by $\pi \cdots \pi$ Interactions

Víctor Blanco, Dolores Abella, Elena Pía, Carlos Platas-Iglesias, Carlos Peinador,* and José M. Quintela*

Departamento de Química Fundamental, Facultad de Ciencias, Universidade da Coruña, Campus A Zapateira, 15071 A Coruña, Spain

Received November 21, 2008

Dinuclear metallo-cycles were assembled from an L-shaped bidentate ligand based on 4,4'-bipyridine and palladium or platinum square-planar *cis* complexes. The palladium (**4a,b**) or platinum (**5a,b**) square metallo-cycles were obtained as 1:1 regioisomeric mixtures depending on which pair of coordinative nitrogen atoms binds to the metal center. The squares display a π -deficient cavity suitable to incorporate two π -donor aromatic systems. Therefore, the reaction with macrocyclic polyethers (BPP34C10 or DN38C10) resulted in the regioselective self-assembly of the [3]catenanes **4a**(BPP34C10 or DN38C10)₂ · 6PF₆ and **5a**(BPP34C10 or DN38C10)₂ · 6PF₆ because only macrocycles **4a** and **5a** present the correct disposition of the π -deficient aromatic systems to maximize the $\pi \cdots \pi$ stacking interactions. Single-crystal X-ray analyses of [3]catenanes revealed that the structures are additionally stabilized by [C–H \cdots O], [N–H \cdots O] bonds and [C–H \cdots π] interactions. The 1:2 inclusion complexes of metallo-cycles were prepared by self-assembly of three components: the ligand 1-(4-(pyridin-4-yl)benzyl)-4,4'-bipyridin-1-ium, a square planar complex M(en)(NO₃)₂ (M = Pd or Pt, en = ethylenediamine), and a dioxoaromatic guest in a 2:2:2 ratio. The comparative study of the formation of 1:2 inclusion complexes has allowed us to conclude that the $\pi \cdots \pi$ interactions between the host and guests are responsible for the observed regioselectivity.

Introduction

Catenanes, molecular systems composed of two or more interlocked macrocycles,¹ have attracted much attention in recent years not only because of their intrinsic beauty or synthetic challenges that their preparation represent but also because of their potential switching properties.² Although the first attempts based on the statistical approach³ or directed syntheses⁴ were not promising, the development of Supramolecular Chemistry allowed efficient syntheses of a very wide variety of interlocked molecular systems. Control over non-covalent interactions such as hydrogen bonding, $\pi \cdots \pi$ stacking, hydrophobic forces, and coordinative bonds has

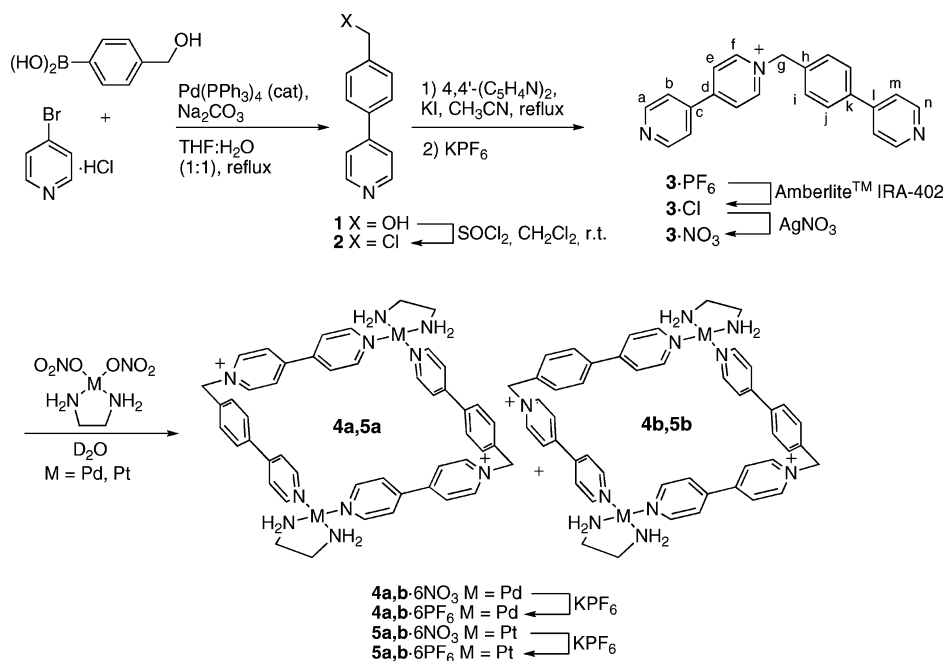
been the key to the success of synthetic strategies based on self-assembly processes.⁵ Therefore, fine-tuning and fully understanding of how these subtle interactions govern the self-assembly processes can be very helpful to design new supramolecular assemblies. As in the classical covalent synthetic chemistry the stereo- and regioselectivity must be understood and controlled, this type of control over the self-assembly processes also is necessary.

Recently, we have reported a stereoselective self-assembly induced by aromatic guests where [C–H \cdots π] interactions

* To whom correspondence should be addressed. E-mail: capeveqo@udc.es.

(1) (a) *Molecular Catenanes, Rotaxanes and Knots*; Sauvage, J.-P., Dietrich-Buchecker, C., Eds.; Wiley-VCH: Weinheim, 1999. (b) For review articles, see Amabilino, D. B.; Stoddart, J. F. *Chem. Rev.* **1995**, *95*, 2725. (c) Chambron, J.-C.; Dietrich-Buchecker, C.; Sauvage, J.-P. In *Templating Self-Assembly, and Self-Organisation*; Sauvage, J.-P., Hosseini, M. W., Eds.; Comprehensive Supramolecular Chemistry Vol. 9; Pergamon: New York, 1996; pp 43–83. (d) Breault, G. A.; Hunter, C. A.; Mayers, P. C. *Tetrahedron* **1999**, *55*, 5265. (e) Vögtle, F.; Dünwald, T.; Schmidt, T. *Acc. Chem. Res.* **1996**, *29*, 451.

(2) (a) Kay, E. R.; Leigh, D. A.; Zerbetto, F. *Angew. Chem., Int. Ed.* **2007**, *46*, 72. (b) Collier, C. P.; Mattersteig, G.; Wong, E. W.; Luo, Y.; Beverly, K.; Sampaio, J.; Raymo, F. M.; Stoddart, J. F.; Heath, J. R. *Science* **2000**, *289*, 1172. (c) Browne, W. R.; Feringa, B. L. *Nat. Nanotechnol.* **2006**, *1*, 25. (d) Balzani, V.; Credi, A.; Venturi, M. *Molecular Devices and Machines - A journey into the Nano World*; Wiley-VCH: Weinheim, 2003. (e) Payer, D.; Rauschenbach, S.; Malinowski, N.; Konuma, M.; Virojanadara, C.; Starke, U.; Dietrich-Buchecker, C.; Collin, J.-P.; Sauvage, J.-P.; Lin, N.; Kern, K. *J. Am. Chem. Soc.* **2008**, *130*, 15662. (3) (a) Wasserman, E. *J. Am. Chem. Soc.* **1960**, *82*, 4433. (b) Frish, H. L.; Wasserman, E. *J. Am. Chem. Soc.* **1961**, *83*, 3789. (c) Agam, G.; Zilkha, A. *J. Am. Chem. Soc.* **1976**, *98*, 5214. (4) Schill, G. *Catenanes, Rotaxanes and Knots*; Academic Press: New York, 1971.

Scheme 1. Synthesis of the Metallochromes **4a,b** and **5a,b**

between the guest and the host play an important role, so that a careful selection of the guest allows the stereoselective self-assembly of atropisomeric Pd(II) metallochromes containing quinoline moieties.⁶ Thus, the metallochromic receptor can adapt the size and shape of its cavity to maximize the interactions with the guest. Despite the fact that there are now numerous examples reported in the literature describing stereoselectively self-assembled systems,⁷ the study of the regioselectivity in self-assembly processes has remained largely unexplored.⁸ Continuing our studies on the synthesis of catenanes and inclusion complexes taking advantage of metal-directed self-assembly,⁹ we decided to investigate if π -donor/ π -acceptor interactions can direct regioselectively a catenation process. Herein, we propose an approach composed of a dynamic system of two regioisomeric square hosts based on an unsymmetrical bidentate ligand; a careful choice of π -complementary guests should allow us to study

the regioselectivity and provide insights into the interactions that govern the process.

Results and Discussion

The precursor of ligand **3** was synthesized by chlorination of 4'-hydroxymethylphenyl-4-pyridine (**1**) obtained by a Suzuki coupling between 4-hydroxymethylphenylboronic acid and 4-bromopyridine (Scheme 1). The reaction of compound **2** with 4,4'-bipyridine in acetonitrile gave the ligand **3** $\cdot PF_6$ after counterion exchange.

Addition of 1 equiv of Pd(en)(NO₃)₂ to a solution of bipyridinium ligand **3** $\cdot NO_3$ (10 mM) at room temperature resulted in the expected formation of the two square metallochromes in a about 1:1 ratio as can be seen from inspection of the 1D and 2D NMR data either in D₂O (**4a,b** $\cdot 6NO_3$) or CD₃CN (**4a,b** $\cdot 6PF_6$, after counterion exchange) solutions (Scheme 1). The ¹³C NMR spectrum (in both solvents) shows the characteristic downfield shiftings expected for coordination of the pyridyl nitrogen atoms to the Pd atom (Table 1). The composition of the mixture remained unchanged in the 0.5–5 mM (D₂O) and 1–5 mM

- (5) (a) Tseng, H.-R.; Vignon, S. A.; Celestre, P. C.; Perkins, J.; Jeppesen, J. O.; Di Fabio, A.; Ballardini, R.; Gandolfi, M. T.; Venturi, M.; Balzani, V.; Stoddart, J. F. *Chem.-Eur. J.* **2004**, *10*, 155, and references therein. (b) Venturini, A.; Wilson, A. J.; Wong, J. K. Y.; Zerbetto, F. *Chem.-Eur. J.* **2004**, *10*, 4960. (c) Jager, R.; Vogtle, F. *Angew. Chem., Int. Ed.* **1997**, *36*, 930. (d) Sauvage, J.-P. *Acc. Chem. Res.* **1998**, *31*, 611, and references therein. (e) Collin, J.-P.; Heitz, V.; Bonnet, S.; Sauvage, J.-P. *Inorg. Chem. Commun.* **2005**, *8*, 1063. (f) Chambron, J.-C.; Collin, J.-P.; Heitz, V.; Jouvenot, D.; Kern, J.-M.; Mobian, P.; Pomeranc, D.; Sauvage, J.-P. *Eur. J. Org. Chem.* **2004**, 1627. (g) Fujita, M.; Fujita, N.; Ogura, K.; Yamaguchi, K. *Nature* **1999**, *400*, 52. (h) Abedin, T. S. M.; Thompson, L. K.; Miller, D. O. *Chem. Commun.* **2005**, 5512. (i) McArdle, C. P.; Irwin, M. J.; Jennings, M. C.; Vittal, J. J.; Puddephatt, R. J. *Chem.-Eur. J.* **2002**, *8*, 723. (j) Westcott, A.; Fisher, J.; Harding, L. P.; Rizkallah, P.; Hardie, M. J. *J. Am. Chem. Soc.* **2008**, *130*, 2950. (k) Liu, Y.; Bruneau, A.; He, J.; Abliz, Z. *Org. Lett.* **2008**, *10*, 765–768. (l) Ghosh, K.; Yang, H.-B.; Northrop, B. H.; Lyndon, M. M.; Zheng, Y.-R.; Muddiman, D. C.; Stang, P. J. *J. Am. Chem. Soc.* **2008**, *130*, 5320–5334. (m) Yang, H.-B.; Ghosh, K.; Northrop, B. H.; Zheng, Y.-R.; Lyndon, M. M.; Muddiman, D. C.; Stang, P. J. *J. Am. Chem. Soc.* **2007**, *129*, 14187–14189.
- (6) Abella, D.; Blanco, V.; Pía, E.; Chas, M.; Platas-Iglesias, C.; Peinador, C.; Quintela, J. M. *Chem. Commun.* **2008**, 2879–2881.

- (7) For example see: (a) Capó, M.; Saá, J. M.; Alvarez, A. *Chem. Commun.* **2002**, 1982. (b) Ohashi, M.; Yagyu, A.; Yamagata, T.; Mashima, K. *Chem. Commun.* **2007**, 3103. (c) Telfer, S. G.; Kuroda, R. *Chem.-Eur. J.* **2005**, *11*, 57. (d) Kiehne, U.; Weilandt, T.; Lützen, A. *Org. Lett.* **2007**, *9*, 1283. (e) Khlobystov, A. N.; Brett, M. T.; Blake, A. J.; Champness, N. R.; Gill, P. M. W.; O'Neill, D. P.; Teat, S. J.; Wilson, C.; Schröder, M. *J. Am. Chem. Soc.* **2003**, *125*, 6753. (f) Wang, R.; Xu, L.; Ji, J.; Shi, Q.; Li, Y.; Zhou, Z.; Hong, M.; Chan, A. S. C. *Eur. J. Inorg. Chem.* **2005**, 751.
- (8) (a) Constable, E. C.; Houghton, I. A.; Housecroft, C. E.; Neuburger, M.; Schaffner, S.; Whall, L. A. *Inorg. Chem. Commun.* **2004**, *7*, 1128. (b) Bogdan, A.; Vysotsky, M. O.; Ikai, T.; Okamoto, Y.; Böhmer, V. *Chem.-Eur. J.* **2004**, *10*, 3324. (c) Alajarin, M.; Pastor, A.; Orenes, R.-A.; Steed, J. W.; Arakawa, R. *Chem.-Eur. J.* **2004**, *10*, 1383.
- (9) (a) Chas, M.; Pía, E.; Toba, R.; Peinador, C.; Quintela, J. M. *Inorg. Chem.* **2006**, *45*, 6117. (b) Chas, M.; Abella, D.; Blanco, V.; Pía, E.; Blanco, G.; Fernández, A.; Platas-Iglesias, C.; Peinador, C.; Quintela, J. M. *Chem.-Eur. J.* **2007**, *13*, 8572.

Table 1. ^1H and ^{13}C NMR Chemical Shift Data ($\Delta\delta$) for Metalloccycles **4a,b** (5 mM), Catenanes **4a**(BPP34C10) $_2$ ·6PF $_6$ (5 mM) and **4a**(DN38C10) $_2$ ·6PF $_6$ (1 mM), and **4a(9b)** $_2$ ·6NO $_3$ (5 mM)^a

| | | a | b | c | d | e | f | g | h | i | j | k | l | m | n |
|--------------------------------------------------|-----------------|-------|-------|----------|----------|-------|----------|-------|-----|-------|-------|----------|------|-------|-------|
| 4a,b ·6PF $_6$ ^b | ^1H | 0.03 | 0.09 | | | -0.14 | -0.02 | -0.04 | | -0.04 | -0.13 | | | -0.01 | -0.01 |
| | ^{13}C | 1.6 | 3.2 | 3.7 | -3.1 | 0.4 | 0.3 | 0.2 | 1.5 | 0.4 | 0.0 | -2.4 | 1.8 | 1.9 | 2.9 |
| 4a (BPP34C10) $_2$ ·6PF $_6$ ^c | ^1H | -0.10 | -0.70 | | | -0.71 | -0.07 | -0.09 | | 0.17 | 0.03 | | | 0.11 | 0.26 |
| | ^{13}C | -0.7 | -1.9 | -3.7 | -3.9 | -2.5 | -0.5 | -0.2 | 0.4 | 0.3 | -0.1 | 0.1 | 0.0 | 0.5 | 0.6 |
| 4a (DN38C10) $_2$ ·6PF $_6$ ^c | ^1H | -0.04 | -1.70 | | | -1.91 | -0.20 | -0.10 | | 0.30 | 0.25 | | | 0.36 | 0.38 |
| | ^{13}C | -1.0 | -2.6 | <i>d</i> | <i>d</i> | -4.9 | <i>d</i> | 0.1 | 0.4 | 0.6 | 0.1 | <i>d</i> | 0.2 | 0.1 | 0.6 |
| 4a,b ·6NO $_3$ ^b | ^1H | 0.16 | 0.04 | | | -0.14 | -0.01 | -0.07 | | -0.06 | -0.19 | | | -0.27 | 0.0 |
| | ^{13}C | 2.2 | 2.5 | 2.6 | -2.8 | 0.2 | 0.1 | 0.5 | 0.5 | -0.9 | -0.4 | -0.9 | -1.9 | 0.8 | 5.8 |
| 4a(9b) $_2$ ·6NO $_3$ ^c | ^1H | -0.17 | -0.93 | | | -1.09 | -0.33 | -0.18 | | 0.31 | 0.46 | | | 0.53 | 0.43 |
| | ^{13}C | -0.6 | -1.6 | -3.6 | -3.8 | -2.0 | -1.4 | -0.1 | 0.3 | 1.7 | 0.2 | -0.2 | -0.3 | 0.0 | 0.7 |

^a Hydrogen and carbon labels (a–n) are defined in Scheme 1. ^b The δ values are compared to those of the free ligand **3**·NO $_3$ or **3**·PF $_6$. ^c The δ values are compared to those of the free metallocycle. ^d Not assigned. ^e Only the data for **4a(9b)** $_2$ ·6NO $_3$ are presented, the values for the remaining inclusion complexes are similar.

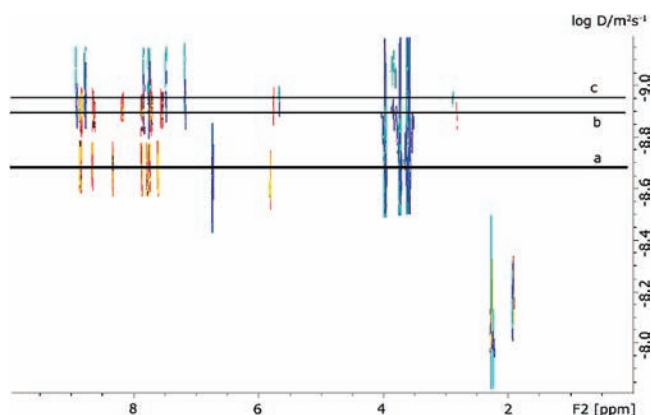


Figure 1. Superposed DOSY (CD $_3$ CN, 500 MHz, 298 K) experiments of (a) ligand **3**·PF $_6$ (10 mM) (red and yellow), (b) **4a,b**·6PF $_6$ (5 mM) (red and yellow), (c) **4a,b**·6PF $_6$ (5 mM) + BPP34C10 (50 mM) (blue).

(CD $_3$ CN) range; below the 1 mM limit in CD $_3$ CN, appreciable amounts of free ligand **3** are detected. To support the binding of the ligand **3** to the metal center, a DOSY (diffusion ordered spectroscopy) experiment was carried out.¹⁰ The results showed that the two species formed have a very similar diffusion coefficient which is significantly smaller than those of ligand **3**·PF $_6$ (Figure 1). The analogous platinum metallocycles were prepared in a similar way. A 1:1 mixture of two regioisomers was obtained upon heating at 100 °C a solution of **3**·NO $_3$ and Pt(en)(NO $_3$) $_2$ in water. In contrast to the palladium metallocycles, this mixture remained stable below the concentration limit of 1 mM in a CD $_3$ CN solution (after counterion exchange) as could be expected from the less labile N–Pt coordinative bond.

The assignment of products **5a,b**·6PF $_6$ as metallocycles was also made based on ESI-HRMS studies where multiply charged intact molecular ions were observed. For example, the experimental isotopic distribution for the ion [**5a,b**·3PF $_6$] $^{3+}$ fits very well with the theoretical calculation (see Supporting Information).

Self-Assembly and NMR Study of [3]Catenanes 4a(BPP34C10 or DN38C10) $_2$ ·6PF $_6$ and 5a(BPP34C10 or DN38C10) $_2$ ·6PF $_6$. A priori, the combination of metallocycles **4a,b** with BPP34C10 could give rise to three

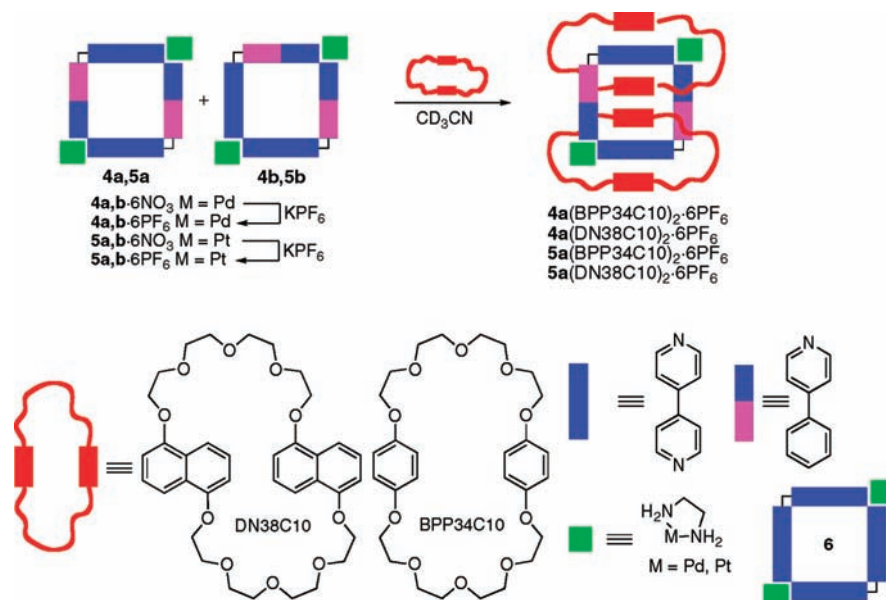
reasonable catenane structures, two [3]catenanes derived from metallocycle **4a**, depending on whether the internal dioxoaryl groups are parallel or perpendicular to the 4,4'-bipyridine moieties (BIPY), and the third [3]catenane derived from **4b**. Although both metallocycles have a quite similar cavity dimensions, only the square **4a** presents the correct BIPY disposition to maximize the $\pi\cdots\pi$ stacking interactions, which are expected to be stronger with the bipyridinium moieties than with the phenylpyridine ones. To check this, we have performed density functional theory (DFT) calculations at the BH&H/6-31+G(d) level (see Supporting Information for computational details). This computational approach has been shown to give a binding energy for the parallel displaced benzene dimer in good agreement with the best available high-level calculations reported in the literature, and qualitatively reproduces the local MP2 potential energy surface of the parallel-displaced benzene dimer.¹¹ Calculations were performed in the model stacked systems (MeBIPY $^+$)(DMB) $_2$ and (TPy)(DMB) $_2$, [where DMB = 1,4-dimethoxybenzene, TPy = 4-*p*-tolylpyridine and MeBIPY $^+$ = *N*-methyl-4,4'-bipyridinium]. Our calculations provide counterpoise-corrected¹² binding energies of 112.8 and 56.0 kJ·mol $^{-1}$ for (MeBIPY $^+$)(DMB) $_2$ and (TPy)(DMB) $_2$, respectively. The inclusion of solvent effects (acetonitrile) results in binding energies of 44.6 and 22.7 kJ·mol $^{-1}$, respectively. Thus, our calculations confirm that the bipyridinium moieties provide stronger $\pi\cdots\pi$ stacking interactions than the phenylpyridine ones, and therefore, the addition of a π -complementary aromatic guest (BPP34C10 or DN38C10) to a solution of **4a,b**·6PF $_6$ in acetonitrile should induce the regioselective formation of the catenane structures derived from **4a** (Scheme 2).

The ^1H NMR spectrum, recorded upon the addition of 5 equiv of BPP34C10 to a solution of **4a,b**·6PF $_6$ in acetonitrile, shows two sets of signals, one attributable to the [3]catenane and the other to the excess of free macrocycle BPP34C10. The 1:4 integration ratio between the aromatic signals of the metallomacrocycle and the cyclophane BPP34C10 indicates that, for each hexacationic square, there are two encircling cyclophane rings in keeping with the molecular structure of a [3]catenane. The diffusion coefficients obtained from

(10) (a) Giuseppone, N.; Schmitt, J.-L.; Allouche, L.; Lehn, J.-M. *Angew. Chem., Int. Ed.* **2008**, *47*, 2235. (b) Otto, W. H.; Keefe, M. H.; Splan, K. E.; Hupp, J. T.; Larive, C. K. *Inorg. Chem.* **2002**, *41*, 6172. (c) Cohen, Y.; Avram, L.; Frish, L. *Angew. Chem., Int. Ed.* **2005**, *44*, 520.

(11) Waller, M. P.; Robertazzi, A.; Platts, J. A.; Hibbs, D. E.; Williams, P. A. *J. Comput. Chem.* **2006**, *27*, 491.

(12) Bernardi, F.; Boys, S. F. *Mol. Phys.* **1970**, *19*, 553.

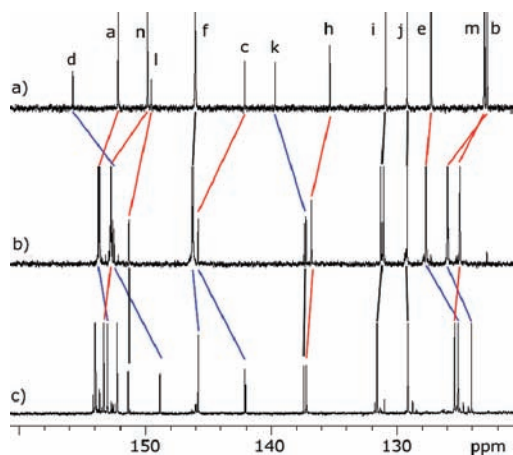
Scheme 2. Synthesis of Catenanes (**4a** or **5a**)(BPP34C10)₂·6PF₆ and (**4a** or **5a**)(DN38C10)₂·6PF₆


DOSY experiments of catenane **4a**(BPP34C10)₂·6PF₆ and metallocycles **4a,b**·6PF₆ showed that the catenane is significantly larger than its components. When the metallocycle and the macrocycle BPP34C10 form part of the catenane, their signals showed the same diffusion coefficients indicating that these components diffuse as a whole. In contrast, the excess of free BPP34C10 displayed a significantly larger diffusion coefficient than that of **4a**(BPP34C10)₂·6PF₆ (Figure 1). One set of signals for the metallocycle is observed in the ¹H NMR spectrum indicating that only one of the two squares is present in the catenane structure. The protons and carbons of the bipyridines are shifted upfield (Table 1 and blue lines in Figure 2) from those of the free metallocycle **4a,b** as a result of the shielding effect of the cyclophane BPP34C10. On the contrary, the protons and carbons of the 4-phenylpyridine (PHPY) moiety are shifted downfield (Table 1 and red lines in Figure 2) suggesting a weak [C–H···π] interaction between the pyridine, the phenyl rings, and the protons of the inside hydroquinol rings. The sign and magnitude of these shifts clearly indicate that the

hydroquinol rings inside the cavity are parallel to the 4,4'-bipyridine systems and orthogonal to the phenylpyridines, resulting in the formation of only one of the two isomeric catenanes of **4a**. Exchange between the “inside” and “along-side” hydroquinol rings in the [3]catenane is fast at room temperature, resulting in an average signal ($\delta = 5.22$ ppm) for the aromatic protons of BPP34C10.

The addition of 2 equiv of naphthalene derivative DN38C10 to a solution of **4a,b** was enough to achieve the reorganization to the single catenane **4a**(DN38C10)₂·6PF₆. The upfield shifts experienced by the bipyridine nuclei are more pronounced in this system (Table 1) because of the better π -donor characteristics of DN38C10. Taking into account the successful use of dibenzo-24-crown-8 (DB24C8) in a similar catenation process with metallocycle **6** (Scheme 2),¹³ it was surprising to verify that no catenation is occurring upon the addition of DB24C8 to a solution of **4a,b**. The ¹H NMR spectrum showed that the only affected signals were those of the ethylenediamine groups, so it is likely that the two crown ether molecules are located over the Pd(en) corners.¹⁴ On the other hand, the lower tendency to catenate of **4a,b** with DB24C8 compared with the metallocycle **6** was attributed to poorer H-bond donor properties of the methylene groups of metallocycle **4a,b** (C–CH₂–N⁺) over those of the square **6** (N⁺–CH₂–N⁺).

When the same strategy that we used in the preparation of the catenanes **4a**(BPP34C10)₂·6PF₆ and **4a**(DN38C10)₂·6PF₆ was employed, the analogous platinum catenanes were obtained. The reaction between ligand **3**·PF₆, Pt(en)(OTf)₂, and the corresponding cyclophane was carried out in acetonitrile at 55 °C to exploit the “molecular lock” strategy introduced by Fujita.¹⁵ Similar results were obtained when a mixture of metallocycles **5a,b** previously isolated was used


Figure 2. Partial ¹³C NMR (CD₃CN, 125 MHz) spectra of (a) ligand **3**·PF₆, (b) metallocycles **4a,b**·6PF₆, and (c) catenane **4a**(BPP34C10)₂·6PF₆. Peak labels are defined in Scheme 1.

(13) Blanco, V.; Chas, M.; Abella, D.; Peinador, C.; Quintela, J. M. *J. Am. Chem. Soc.* **2007**, *129*, 13978.

(14) This interaction has been previously detected in the catenane **6**(DB24C8)₂ described in ref 13.

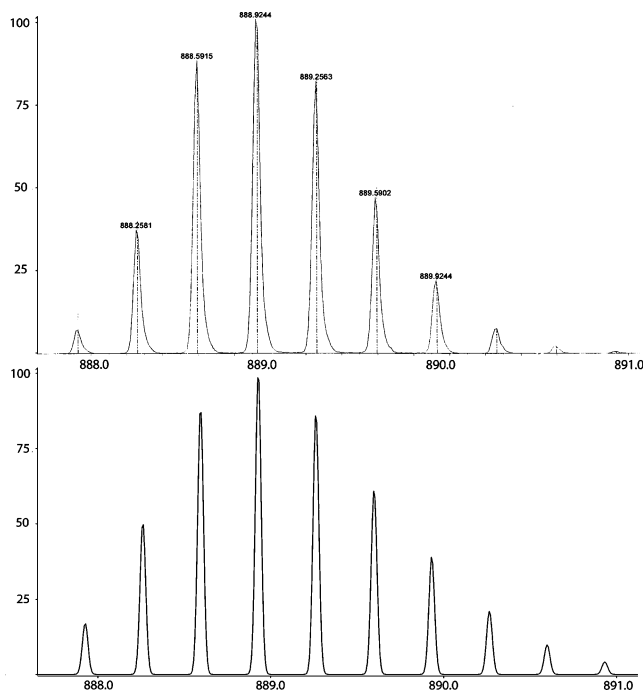


Figure 3. Observed (top) and theoretical (bottom) isotopic distribution for the fragment $[5a(BPP34C10)_2-3PF_6]^{3+}$.

as starting material for the synthesis of the platinum catenanes. The 1H and ^{13}C NMR spectra showed the presence of a unique species with spectroscopic characteristics very similar to the corresponding palladium catenanes suggesting the regioselective catenation of metallocycle **5a** to afford the [3]catenanes **5a**(BPP34C10) $_2$ ·6PF $_6$ and **5a**(DN38C10) $_2$ ·6PF $_6$. Mass spectrometry supported the structure, showing peaks resulting from the loss of between three and five hexafluorophosphate anions. Moreover the high-resolution electrospray mass spectrum of $[5a(BPP34C10)_2-3PF_6]^{3+}$ is reproduced in Figure 3. A comparison between the calculated mass distribution for the triply charged species and the experimental data confirms the authenticity of $[5a(BPP34C10)_2-3PF_6]^{3+}$.

X-ray Crystal Structure of [3]catenanes 4a(BPP34C10) $_2$ and 5a(DN38C10) $_2$. Single crystals of catenane **4a**(BPP34C10) $_2$ suitable for X-ray crystallography were obtained from a solution of ligand **3**·PF $_6$, Pd(en)OTf $_2$, and BPP34C10 in acetonitrile (Table 2). The crystal structure shows that the molecule has crystallographic C_i symmetry, with the hexacationic metallocycle interlocked by two molecules of cyclophane BPP34C10, showing a parallel $\pi\cdots\pi$ stacking disposition of six aromatic systems: HQ $_{out}$ /BIPY/HQ $_{in}$ /HQ $_{in}$ /BIPY/HQ $_{out}$, where HQ $_{out}$ and HQ $_{in}$ stand for the alongside and the inside hydroquinol rings, respectively (Figure 4). As a consequence, the pyridine rings of bipyridines are almost coplanar (torsional angle 4°), while the 4-phenylpyridine system has a torsional angle of 42°. The interplanar separation HQ $_{in}$ -HQ $_{in}$ is 3.50 Å, and the distance between their centroids is 4.38 Å; hence one HQ $_{in}$

is displaced 2.63 Å with respect to the other. The distances HQ $_{in}$ /BIPY and BIPY/HQ $_{out}$ are 3.53 Å and 3.52 Å, respectively, indicating $\pi\cdots\pi$ interaction between these systems. In addition to the habitual [C–H \cdots O] bonds¹⁶ between the α -CH bipyridine hydrogens and the oxygen atoms of BPP34C10, [N–H \cdots O] hydrogen bonds between amine protons and the oxygen atoms of the polyether chain are also detected.¹⁷ The dimensions of the metallocycle are 15.50 × 14.34 Å (palladium–palladium and methylene–methylene distances, respectively).

The crystal structure of **5a**(DN38C10) $_2$ (Table 2) shows that the molecule has crystallographic C_i symmetry, with a parallel $\pi\cdots\pi$ stacking disposition of six aromatic systems with interplanar distances between 3.4 Å and 3.5 Å. In addition, the catenane is stabilized by [N–H \cdots O] bonds between ethylenediamine nitrogens and polyether oxygens, [C–H \cdots O] bonds between the α -CH pyridine and $^+NCH_2$ group hydrogens and the oxygen atoms of DN38C10, and [C–H $\cdots\pi$] interactions between hydrogen atom on the C-4 position of the naphthalene moiety located inside the metallocycle and the pyridine ring of the PHPY system (Figure 5). Although the 1,5-dialkoxynaphthalene derivatives are better π -donors than hydroquinone derivatives, the dihedral angle of the BIPY is 18°, slightly larger than that of **4a**(BPP34C10) $_2$. The PHPY system is distorted from the normal planar geometry, involving both twisting (12°) and bowing¹⁸ (20°) of their aromatic rings.

Self-Assembly and NMR Study of 1:2 Inclusion Complexes 4a(9b–11b) $_2$ ·6NO $_3$. Although the structure of catenanes is unambiguously characterized, the reason of the regioselectivity should be addressed. With the aim of clarifying this issue, we carried out a series of experiments to establish the interactions between the components that govern the preferred formation of the catenanes **4a**(BPP34C10) $_2$ ·6PF $_6$ and **4a**(DN38C10) $_2$ ·6PF $_6$. A unique self-assembled structure can be formed only if it is strongly favored over the others thermodynamically.

Recently, we have reported¹⁹ the formation of 1:2 inclusion complexes between the symmetric metallocycle **6** and dihydroxyaromatic guests. Thus as could be expected, the addition of the guests **7–12** to a solution of **4a,b**·6NO $_3$ in D $_2$ O resulted in the partial or total reorganization of the *incorrect* metallocycle **4b**·6NO $_3$ to yield the 1:2 inclusion complexes of **4a**·6NO $_3$ (Scheme 3 and Table 3). Obviously, the mechanism requires, as in the case of catenanes, the dissociation of the N atoms from the palladium centers. In contrast to the catenanes, in these cases the inclusion equilibrium between the complexed species and its separated

(15) (a) Fujita, M.; Ibukuro, F.; Yamaguchi, K.; Ogura, K. *J. Am. Chem. Soc.* **1995**, *117*, 4175. (b) Hori, A.; Kataoka, H.; Okano, T.; Sakamoto, S.; Yamaguchi, K.; Fujita, M. *Chem. Commun.* **2002**, 182. (c) Yamashita, K.-i.; Kawano, M.; Fujita, M. *J. Am. Chem. Soc.* **2007**, *129*, 1850.

(16) See for example: (a) Ashton, P. R.; Ballardini, R.; Balzani, V.; Credi, A.; Gandolfi, M. T.; Menzer, S.; Perezgarcia, L.; Prodi, L.; Stoddart, J. F.; Venturi, M.; White, A. J. P.; Williams, D. J. *J. Am. Chem. Soc.* **1995**, *117*, 11171. (b) Asakawa, M.; Ashton, P. R.; Balzani, V.; Brown, C. L.; Credi, A.; Matthews, O. A.; Newton, S. P.; Raymo, F. M.; Shipway, A. N.; Spencer, N.; Quick, A.; Stoddart, J. F.; White, A. J. P.; Williams, D. J. *Chem.—Eur. J.* **1999**, *5*, 860.

(17) Distances [H \cdots O] and [N \cdots O], and angle [N–H \cdots O]: (a) 2.31, 3.04 Å, 135° and (b) 2.22, 2.99 Å, 142°.

(18) The bowing of the PHPY residue is expressed by the angle subtended by the CH $_2$ -C $_6$ H $_4$ and N-Pt bonds emanating from the PHPY system.

(19) Blanco, V.; Chas, M.; Abella, D.; Pia, E.; Platas-Iglesias, C.; Peinador, C.; Quintela, J. M. *Org. Lett.* **2008**, *10*, 409.

Table 2. X-ray Crystallographic Experimental Data of Catenanes **4a**(BPP34C10)₂•6OTf and **5a**(DN38C10)₂•4OTf•2PF₆^a

| | 4a (BPP34C10) ₂ •6OTf | 5a (DN38C10) ₂ •4OTf•2PF ₆ |
|------------------------------------------------|------------------------------------------------------------------------------------------------------------------|---------------------------------------------------------------------------------------------------------------------------------|
| empirical formula | C ₁₁₀ H ₁₂₀ F ₁₈ N ₁₀ O ₃₈ Pd ₂ S ₆ | C ₁₂₄ H ₁₄₀ F ₂₄ N ₁₀ O ₃₂ P ₂ Pt ₂ S ₄ |
| formula weight | 2937.41 | 3350.92 |
| crystal system | monoclinic | monoclinic |
| space group | <i>P</i> 2 ₁ / <i>n</i> | <i>P</i> 2 ₁ / <i>n</i> |
| <i>a</i> (Å) | 15.496(3) | 16.663(5) |
| <i>b</i> (Å) | 20.953(4) | 22.104(5) |
| <i>c</i> (Å) | 20.969(4) (5) | 21.824(5) |
| α (deg) | 90 | 90 |
| β (deg) | 95.940(4) | 108.403(5) |
| γ (deg) | 90 | 90 |
| <i>V</i> (Å ³) | 6772(2) | 7627(3) |
| <i>Z</i> | 2 | 2 |
| <i>D</i> _{calcd} (Mgm ⁻³) | 1.527 | 1.459 |
| <i>μ</i> (mm ⁻¹) | 0.466 | 2.005 |
| <i>F</i> (000) | 3208 | 3396 |
| crystal size (mm) | 0.56 × 0.35 × 0.20 | 0.13 × 0.08 × 0.07 |
| θ limits (deg) | 1.32 to 26.02 | 1.35 to 25.04 |
| <i>hkl</i> limits | −19,19/0,25/0,25 | −19,18/−26,26/−17,25 |
| reflections collected | 13318 | 57442 |
| independent reflections | 13318 [<i>R</i> _{int} = 0.0000] | 13437 [<i>R</i> _{int} = 0.0797] |
| max and min transmission | 0.9125 and 0.7802 | 0.8724 and 0.7806 |
| goodness-of-fit on <i>F</i> ² | 1.066 | 1.073 |
| <i>R</i> [<i>I</i> > 2σ(<i>I</i>)] | <i>R</i> 1 = 0.0624 <i>wR</i> 2 = 0.1282 | <i>R</i> 1 = 0.0631 <i>wR</i> 2 = 0.1774 |
| <i>R</i> (all data) | <i>R</i> 1 = 0.1059 <i>wR</i> 2 = 0.1527 | <i>R</i> 1 = 0.1136 <i>wR</i> 2 = 0.2209 |

^a In common: Refinement method, full-matrix least-squares on *F*². Wavelength 0.71073 Å. Temperature 100(2) K. Absorption correction method: multi scan.

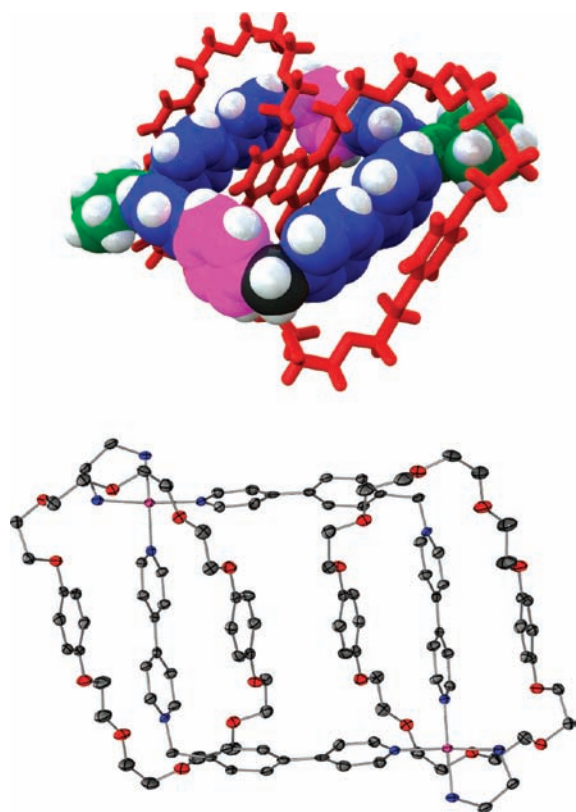


Figure 4. Top: space-filling view of the X-ray structure of catenane **4a**(BPP34C10)₂•6OTf. The color labeling scheme is as follow: pyridine rings (blue), phenylene groups (pink), Pd(en) (green), methylene groups of the metallocycle (black), and BPP34C10 (red). Solvent molecules and counterions have been omitted for clarity. Bottom: ORTEP drawing of **4a**(BPP34C10)₂•6OTf showing thermal ellipsoids at 50% probability.

components is fast in the ¹H NMR time scale so only averaged signals are detected. The DOSY experiment of a solution of **4a,b**•6NO₃ and 2 equiv of **9b** in D₂O showed

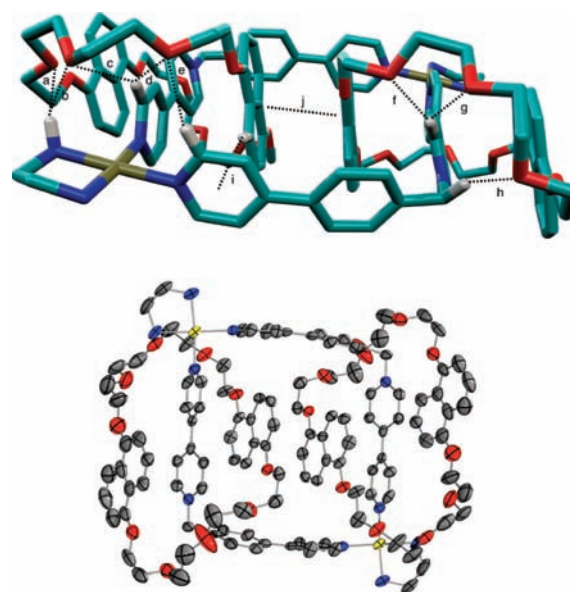
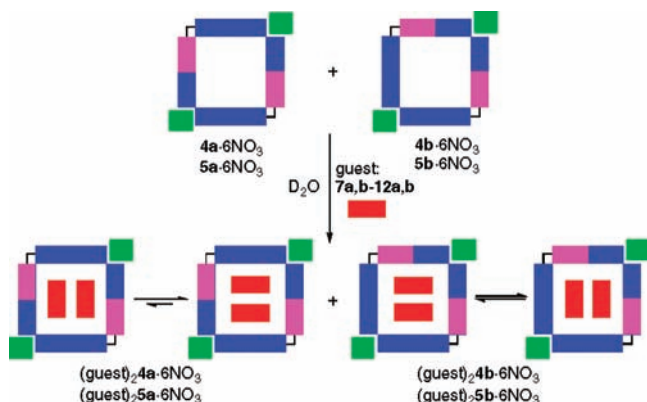


Figure 5. Top: crystal structure of [3]catenane **5a**(DN38C10)₂ showing [N–H···O] bonds (a, b, [H···O] and [N···O] distances and [N–H···O] angle): a 2.61, 3.34 Å, 136°; b 2.22, 3.03 Å, 145°, [C–H···O] bonds (c–h, [H···O] and [C···O] distances and [C–H···O] angle): c 2.50, 3.31 Å, 143°; d 2.47, 3.27 Å, 142°; e 2.45, 3.26 Å, 144°; f 2.41, 3.29 Å, 154°; g 2.97, 3.80 Å, 146°; h 2.49, 3.42 Å, 157°, [C–H···π] (i, [H···centroid] and [C···centroid] distances and [C–H···centroid] angle): i 2.83, 3.67 Å, 147°, and π···π interactions (j, interplanar distance): j 3.52 Å. Solvents molecules, counterions and hydrogen atoms have been omitted for clarity. Bottom: ORTEP drawing of **5a**(DN38C10)₂ showing thermal ellipsoids at 50% probability.


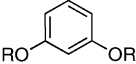
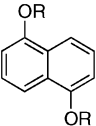
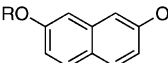
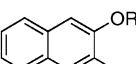
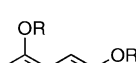
that the diffusion coefficient for the guest signals is intermediate between those of free **9b** and metallocycles **4a,b**•6NO₃ (see Supporting Information). The self-assembly of the guests **9b–11b** and **4a,b**•6NO₃ in D₂O solutions gave exclusively the inclusion complex of metallocycle **4a**. Most of the spectroscopic characteristics of **4a(9b–11b)**•6NO₃

Scheme 3. Schematic Representation of Inclusion Complexes (**4a** or **5a**)(guest)₂•6NO₃ and (**4b** or **5b**)(guest)₂•6NO₃



are quite similar to those of the previously described catenanes. For example, the ¹H and ¹³C NMR spectra of **4a(9b)**₂•6NO₃ showed the characteristic upfield shiftings of the signals of the BIPY systems and the slight downfield shiftings of the signals of the PHPY (Table 1) indicating that the parallel insertion to BIPYs of the naphthalene systems predominates over the perpendicular one (Scheme 3). Moreover, this assignment is substantiated further by the multiplicity of the ethylene group signals (ethylenediamine)

Table 3. Ratio of Populations [**4a**(guest)₂•6NO₃/**4b**(guest)₂•6NO₃] in D₂O Solutions

| Guest | equiv ^a | Ratio of populations ^b |
|------------------------------------------------------------------------------------------------------|--------------------|-----------------------------------|
| BPP34C10 ^c | 5 | 100/0 |
| DN38C10 ^c | 2 | 100/0 |
| DB24C8 ^c | 2 | 50/50 |
|  7a R = H | 12 | 80/20 |
| 7b R = (CH ₂) ₂ O(CH ₂) ₂ OH | 8 | 84/16 |
|  8a R = H | 12 | 61/39 |
| 8b R = (CH ₂) ₂ O(CH ₂) ₂ OH | 8 | 77/23 |
|  9a R = H | ^d | ^d |
| 9b R = (CH ₂) ₂ O(CH ₂) ₂ OH | 1 | 100/0 |
|  10a R = H | 2 | 90/10 |
| 10b R = (CH ₂) ₂ O(CH ₂) ₂ OH | 2 | 100/0 |
|  11a R = H | 1 | 70/30 |
| 11b R = (CH ₂) ₂ O(CH ₂) ₂ OH | 1 | 100/0 |
|  12a R = H | ^d | ^d |
| 12b R = (CH ₂) ₂ O(CH ₂) ₂ OH | 2 | 90/10 |

^a Number of equiv added until no change in the regioisomers ratio was observed. ^b The populations of both species were determined by integration of their respective peaks in the ¹H NMR spectra. ^c In CD₃CN solution. ^d Because the substrate is very insoluble exclusive formation of the inclusion complexes could not be achieved.

and its correlation in the COSY spectrum, where they display a cross-peak only consistent with **4a(9b)**₂•6NO₃.

As could be expected, when platinum metalocycles **5a,b**•6NO₃ were used instead of **4a,b**•6NO₃ under the same conditions in the formation of inclusion complexes, no regioselectivity was observed. The inertness of the N–Pt bond at low temperatures prevents a fast equilibration between **5a** and **5b**, which is necessary to reach the regioselectivity. Although the inertness of N–Pt bond diminishes when the temperature is increased, a 1:1 mixture of isomeric inclusion complexes of **5a** and **5b** upon heating at 100 or 50 °C was detected by ¹H NMR spectroscopy. In this case, the smaller binding constant at higher temperatures can account for this fact.

The comparison of the results summarized in Table 3 allows us to draw some conclusions. First, cyclic guests (in acetonitrile solution) seem to favor higher regioselectivities than their acyclic counterparts (e.g., BPP34C10 and **7a,b**). Assuming a similar π -donor capacity for the dioxaryl rings of BPP34C10 and **7a,b** and almost identical entropic costs for all the self-assembly processes, then the number and strength of its π -interactions with the metalocycles determine the regioselectivity. Thus, the ratio of π -interaction energies between **4b**(BPP34C10)₂/**4a**(BPP34C10)₂ is smaller than those of the inclusion complexes **4b**(**7a**)₂/**4a**(**7a**)₂ resulting in a higher regioselectivity for the former. Second, naphthalenic substrates achieve higher selectivities than phenylenic derivatives because of their better donor character. Finally, the presence of the polyether chains in the acyclic guest (e.g., **7b**, **8b**, **10b**, and **11b**) increased the regioselectivity only very slightly with respect to the substrates without these chains. These observations clearly support the fact that the $\pi\cdots\pi$ stacking forces are the main source of the regioselectivity.

Conclusions

To summarize, we have demonstrated a facile synthesis of square palladium and platinum metalocycles by the self-assembly between the ligand 1-(4-(pyridin-4-yl)benzyl)-4,4'-bipyridin-1-ium and the square planar complexes M(en)(NO₃)₂ (M = Pd or Pt). It has been shown that the square metalocycles can undergo a regioselective catenation process via the complementary $\pi\cdots\pi$ interactions between the BIPY systems of the metalocycle and the dioxaryl rings of the cyclophane (BPP34C10 or DN38C10). The structure of these [3]catenanes has been studied in solid state and solution. Moreover, we have shown that the square metalocycles are also receptors for acyclic aromatic substrates, the comparative study of the formation of 1:2 inclusion complexes allowing us to conclude that the $\pi\cdots\pi$ interactions between host and guests are responsible for the observed regioselectivity.

Experimental Section

Reagents and Materials. Cyclophanes BPP34C10²⁰ and DN38C10²¹ and compounds **7b**,²⁰ **8b**,²² **9b**,²² **10b**,²³ and **11b**²⁴ were prepared according to published procedures. All other reagents used

(20) Anelli, P. L.; et al. *J. Am. Chem. Soc.* **1992**, *114*, 193.

(21) Amabilino, D. B.; Ashton, P. R.; Balzani, V.; Boyd, S. E.; Credi, A.; Lee, J. Y.; Menzer, S.; Stoddart, J. F.; Venturi, M.; Williams, D. J. *J. Am. Chem. Soc.* **1998**, *120*, 4295.

were commercial grade chemicals from freshly opened containers. Milli-Q water was purified with a Millipore Gradient A10 apparatus. Merck 60 F₂₅₄ foils were used for thin layer chromatography, and Merck 60 (230–400 mesh) silica gel was used for flash chromatography. Proton and carbon nuclear magnetic resonance spectra were recorded on a Bruker Avance 300 or Bruker Avance 500 equipped with a dual cryoprobe for ¹H and ¹³C, using the deuterated solvent as lock and the residual protiated solvent as internal standard. DOSY experiments were referenced using the value $1.92 \times 10^{-9} \text{ m}^2 \text{ s}^{-1}$ for the DHO signal in D₂O at 298 K²⁵ and an arbitrary value $8.32 \times 10^{-9} \text{ m}^2 \text{ s}^{-1}$ for the CHD₂CN signal in CD₃CN at 298 K. Mass spectrometry experiments were carried out in a Thermo MAT95XP spectrometer for low-resolution EI and FAB using thioglycerol or 3-nitrobenzyl alcohol (3-NBA) as matrix (FAB) and a LC-Q-q-TOF Applied Biosystems QSTAR Elite spectrometer for low- and high-resolution ESI. Melting points were measured using Stuart Scientific SMP3 apparatus. Microanalyses for C, H, and N were performed by the elemental analyses general service of the University of A Coruña.

Crystal Structure Analysis. The structures were solved by direct methods and refined with the full-matrix least-squares procedure (SHELX-97)²⁶ against F^2 . The X-ray diffraction data were collected on a Bruker SMART 1k or a Bruker X8 ApexII diffractometer. Non-solvent hydrogen atoms were placed in idealized positions with $U_{\text{eg}}(\text{H}) = 1.2U_{\text{eg}}(\text{C})$ and were allowed to ride on their parent atoms. Solvent hydrogen atoms were placed in idealized positions with $U_{\text{eg}}(\text{H}) = 1.5U_{\text{eg}}(\text{C})$ and were allowed to ride on their parent atoms.

4-(4'-Hydroxymethylphenyl)pyridine (1). To a solution of 4-bromopyridine hydrochloride (2.05 g, 10.5 mmol) in THF/H₂O 1:1 (500 mL) were added 4-(hydroxymethyl)phenylboronic acid (1.60 g, 10.5 mmol), Na₂CO₃ (6.70 g, 63.2 mmol), and palladium tetrakis(triphenylphosphine) (608 mg, 0.53 mmol). The reaction mixture was heated under reflux and an atmosphere of argon for 18 h. After cooling, the solution was concentrated in vacuo to a volume of approximately 250 mL and extracted with CH₂Cl₂ (3 × 150 mL). The combined extracts were dried over anhydrous MgSO₄. Filtration and evaporation of the solvent gave the crude product, which was purified by column chromatography (SiO₂, EtOAc) to yield **1** (1.71 g, 91%) as a white solid. Mp = 171–173 °C. ¹H NMR (300 MHz, CDCl₃) δ: 2.20 (1H, br s); 4.79 (2H, s); 7.50 (4H, m); 7.65 (2H, d, $J = 8.2$ Hz); 8.65 (2H, d, $J = 6.1$ Hz); ¹³C NMR (75 MHz, CDCl₃) δ: 64.7 (CH₂); 121.6 (CH); 127.1 (CH); 127.6 (CH); 137.3 (C); 142.0 (C); 148.0 (C); 150.2 (CH). MS-EI (m/z): 185.15 [M]⁺. Anal. Calcd C₁₂H₁₁NO: C, 77.81; H, 5.99; N, 7.56. Found C, 77.58; H, 5.76; N, 7.72.

4-(4'-Chloromethylphenyl)pyridine (2). To a solution of **1** (1.55 g, 8.37 mmol) in CH₂Cl₂ (300 mL) cooled to 5 °C was added dropwise SOCl₂ (6.1 mL, 84 mmol). The reaction mixture was stirred at room temperature for 18 h. Then, the pH was adjusted to 10 with aqueous ammonia at 5 °C, and water (300 mL) was added. The organic extract was washed with H₂O (3 × 60 mL) and dried over anhydrous MgSO₄. The solvent was removed under reduced

pressure to yield **2** (1.64 g, 96%) as an analytical pure solid. Mp = 83–86 °C (decomp). ¹H NMR (300 MHz, CDCl₃) δ: 4.64 (2H, s); 7.50 (4H, m); 7.64 (2H, d, $J = 8.3$ Hz); 8.67 (2H, d, $J = 5.8$ Hz); ¹³C NMR (75 MHz, CDCl₃) δ: 45.8 (CH₂); 121.7 (CH); 127.5 (CH); 129.5 (CH); 138.4 (C); 138.5 (C); 147.7 (C); 150.4 (CH). MS-EI (m/z): 203.11 [M]⁺; 168.15 [M–Cl]⁺. Anal. Calcd C₁₂H₁₀ClN: C, 70.77; H, 4.95; N, 6.88. Found C, 70.60; H, 4.99; N, 6.63.

1-(4-(Pyridin-4-yl)benzyl)-4,4'-bipyridin-1-ium Hexafluorophosphate (3•PF₆). To a solution of 4,4'-bipyridine (4.60 g, 29.5 mmol) and a catalytic amount of KI in refluxing CH₃CN (50 mL) was slowly added a solution of **2** (1.20 g, 5.89 mmol) cooled to 0 °C in CH₃CN (75 mL). The reaction was refluxed for 18 h; after cooling, the solvent was evaporated in vacuo. The resulting residue was triturated with ethyl ether (5 × 100 mL) to give a crude product which was purified by column chromatography (SiO₂, acetone/NH₄Cl 1.5M/MeOH 5:4:1). The product-containing fractions were combined and the solvents were removed in vacuo. The residue was dissolved in H₂O/CH₃OH (90/10, 300 mL) and an excess of KPF₆ was added until no further precipitation was observed. The solid was filtered and washed with water to give **3•PF₆** (1.40 g, 51%) as a white solid. Mp = 210–212 °C (decomp). ¹H NMR (500 MHz, CD₃CN) δ: 5.82 (2H, s); 7.61 (2H, d, $J = 8.5$ Hz); 7.75 (2H, d, $J = 6.3$ Hz); 7.79 (2H, d, $J = 6.2$ Hz); 7.87 (2H, d, $J = 8.4$ Hz); 8.34 (2H, d, $J = 6.9$ Hz); 8.67 (2H, d, $J = 6.3$ Hz); 8.85 (2H, d, $J = 6.2$ Hz); 8.87 (2H, d, $J = 7.0$ Hz); ¹³C NMR (125 MHz, CD₃CN) δ: 64.6 (CH₂); 122.8 (CH); 123.1 (CH); 127.3 (CH); 129.2 (CH); 130.9 (CH); 135.3 (C); 139.7 (C); 142.1 (C); 146.0 (CH) 149.5 (C); 149.8 (CH); 152.1 (CH); 155.7 (C). MS-ESI (m/z): 324.2 [M–PF₆]⁺. Anal. Calcd C₂₂H₁₈F₆N₃P: C, 56.30; H, 3.87; N, 8.95. Found C, 56.58; H, 3.69; N, 8.84.

1-(4-(Pyridin-4-yl)benzyl)-4,4'-bipyridin-1-ium Nitrate (3•NO₃). A suspension of **3•PF₆** (0.70 g, 1.5 mmol) and Amberlite IRA-402 (7.0 g) in H₂O (100 mL) was stirred at room temperature for 18 h. After filtration over a pad of Celite, the solvent was removed under reduced pressure to yield **3•Cl** (0.52 g, 96%). A solution of **3•Cl** (0.517 g, 1.44 mmol) and AgNO₃ (0.244 g, 1.44 mmol) was stirred at room temperature for 18 h with exclusion of light. After filtration over a pad of Celite, the solvent was removed under reduced pressure to yield **3•NO₃** (0.55 g, 99%). Mp = 181–183 °C (decomp). ¹H NMR (500 MHz, D₂O) δ: 5.94 (2H, s); 7.65 (2H, d, $J = 8.3$ Hz); 7.89 (2H, d, $J = 6.4$ Hz); 7.93 (2H, d, $J = 8.3$ Hz); 8.01 (2H, d, $J = 6.3$ Hz); 8.42 (2H, d, $J = 7.0$ Hz); 8.67 (2H, d, $J = 6.5$ Hz); 8.75 (2H, d, $J = 6.3$ Hz); 9.04 (2H, d, $J = 7.0$ Hz); ¹³C NMR (125 MHz, D₂O) δ: 63.6 (CH₂); 122.5 (CH); 123.4 (CH); 126.2 (CH); 128.6 (CH); 129.8 (CH); 134.9 (C); 137.4 (C); 142.5 (CH); 144.9 (CH) 145.2 (CH); 152.6 (C); 153.4 (C); 154.4 (C). MS-FAB (thioglycerol) (m/z): 324.2 [M–NO₃]⁺. Anal. Calcd C₂₂H₁₈N₄O₃: C, 68.38; H, 4.70; N, 14.50. Found C, 68.12; H, 4.94; N, 14.46.

Metallocomplexes 4a,b•6NO₃. A solution of **3•NO₃** (11.6 mg; 0.030 mmol) and Pd(en)(NO₃)₂ (8.7 mg, 0.030 mmol) in D₂O (3.0 mL) was stirred at room temperature for 1 h. ¹H NMR (500 MHz, D₂O) δ: 2.91 (8H, m); 5.87 (4H, s); 7.59 (4H, m); 7.74 (8H, m); 7.93 (4H, m); 8.28 (4H, m); 8.67 (4H, m); 8.91 (4H, m); 9.03 (4H, m); ¹³C NMR (125 MHz, D₂O) δ: 46.5, 46.5 (CH₂); 46.6, 46.6 (CH₂); 64.1 (CH₂); 124.1, 124.2 (CH); 124.9, 125.0 (CH); 126.4 (CH); 128.2 (CH); 128.9 (CH); 135.4 (C); 136.4, 136.5 (C); 145.0 (CH); 150.6, 150.7 (C); 150.0 (CH); 151.5, 151.6 (C); 152.1 (CH).

Metallocomplexes 4a,b•6PF₆. To a solution of **3•NO₃** (30.9 mg; 0.080 mmol) and Pd(en)(NO₃)₂ (23.2 mg, 0.080 mmol) in H₂O (8.0 mL) was added an excess of KPF₆ until no further precipitation was observed. The solid was filtered and washed with water to give **4a,b•6PF₆** as a white solid (50.2 mg, 93%). Mp = 170–172

- (22) Amabilino, D. B.; Anelli, P. L.; Ashton, P. R.; Brown, G. R.; Córdova, E.; Godínez, L. A.; Hayes, W.; Kaifer, A. E.; Philp, D.; Slawin, A. M. Z.; Spencer, N.; Stoddart, J. F.; Tolley, M. S.; Williams, D. J. *J. Am. Chem. Soc.* **1995**, *117*, 11142.
 (23) Asakawa, M.; Ashton, P. R.; Boyd, S. E.; Brown, C. L.; Gillard, R. E.; Kocian, O.; Raymo, F. M.; Stoddart, J. F.; Tolley, M. S.; White, A. J. P.; Williams, D. J. *J. Org. Chem.* **1997**, *62*, 26.
 (24) Czech, B.; Czech, A.; Bartsch, R. A. *J. Heterocycl. Chem.* **1984**, *21*, 341.
 (25) Longsworth, L. G. *Phys. Chem.* **1960**, 1914.
 (26) Sheldrick, G. M. *SHELX-97, An Integrated System for Solving and Refining Crystal Structures from Diffraction Data*; University of Göttingen: Göttingen, Germany, 1997.

°C (decomp). ^1H NMR (500 MHz, CD_3CN) δ : 2.85 (8H, s); 4.28 (4H, br s); 4.34 (4H, br s); 5.78 (4H, m); 7.57 (4H, m); 7.74 (8H, m); 7.88 (4H, m); 8.20 (4H, m); 8.66 (4H, m); 8.83–8.89 (8H, m); ^{13}C NMR (125 MHz, CD_3CN) δ : 47.7, 47.7 (CH_2); 47.8, 47.9 (CH_2); 64.8 (CH_2); 124.9, 125.0 (CH); 125.9, 126.0 (CH); 127.7, 127.7 (CH); 129.2, 129.2 (CH); 131.1, 131.3 (CH); 136.8 (C); 137.2, 137.4 (C); 145.8, 145.8 (C); 146.2, 146.3 (CH); 151.3, 151.3 (C); 152.5, 152.6 (C); 152.7, 152.7 (CH); 153.6, 153.7 (CH).

Metalloacycles $5\mathbf{a},\mathbf{b}\cdot 6\text{PF}_6$. A solution of ligand $3\cdot\text{NO}_3$ (96.9 mg, 0.250 mmol) and $\text{Pt}(\text{en})(\text{NO}_3)_2$ (94.8 mg, 0.250 mmol) in H_2O was heated at 100 °C for 7 d. Upon cooling to room temperature, an excess of KPF_6 was added until no further precipitation was observed. The solid was filtered to yield $5\mathbf{a},\mathbf{b}\cdot 6\text{PF}_6$ (249.5 mg, 99%) as a white solid. Mp = 180–181 °C (decomp). ^1H NMR (500 MHz, CD_3CN) δ : 2.78 (8H, s); 4.87 (4H, br s); 4.92 (4H, br s); 5.79 (4H, m); 7.58 (4H, m); 7.72–7.79 (8H, m); 7.85–7.90 (4H, m); 8.21–8.25 (4H, m); 8.66–8.70 (4H, m); 8.85–8.92 (8H, m); ^{13}C NMR (125 MHz, CD_3CN) δ : 48.4, 48.5 (CH_2); 64.7 (CH_2); 125.2, (CH); 126.2, 126.3 (CH); 127.5, 127.5 (CH); 129.1, 129.1 (CH); 131.0, 131.1 (CH); 136.7 (C); 136.9, 137.0 (C); 145.5 (C); 146.1, 146.1 (CH); 151.1 (C); 152.1, 152.2 (C); 153.2, 153.3 (CH); 154.3, 154.3 (CH). HRMS-ESI (m/z): Calcd for $[\text{M}-2\text{PF}_6]^{2+}$ 869.1114, found 869.1135; calcd for $[\text{M}-3\text{PF}_6]^{3+}$ 531.0860, found 531.0856. Anal. Calcd $\text{C}_{48}\text{H}_{52}\text{F}_{36}\text{N}_{10}\text{P}_6\text{Pt}_2$: C, 28.41; H, 2.58; N, 6.90. Found C, 28.28; H, 2.79; N, 6.72.

Catenane $4\mathbf{a}(\text{BPP34C10})_2\cdot 6\text{PF}_6$. To a solution of $4\mathbf{a},\mathbf{b}\cdot 6\text{PF}_6$ (5.5 mg, 3.0×10^{-3} mmol) in CD_3CN (0.6 mL) was added BPP34C10 (16.1 mg, 3.0×10^{-3} mmol). ^1H NMR (500 MHz, CD_3CN) δ : 2.89 (8H, s); 3.12–3.23 (16H, m); 3.50–4.10 (m, excess of BPP34C10); 4.43 (4H, br s); 4.53 (4H, br s); 5.22 (16H, br s); 5.67 (4H, s); 6.75 (s, excess of BPP34C10); 7.18 (4H, d, $J = 6.9$ Hz); 7.49 (4H, d, $J = 7.0$ Hz); 7.74 (4H, d, $J = 8.7$ Hz); 7.77 (4H, d, $J = 8.6$ Hz); 7.85 (4H, d, $J = 6.9$ Hz); 7.88 (8H, m); 8.92 (4H, d, $J = 6.9$ Hz); ^{13}C NMR (125 MHz, CD_3CN) δ : 47.8 (CH_2); 48.1 (CH_2); 64.6 (CH_2); 67.7 (CH_2); 68.9 (CH_2 , excess of BPP34C10); 70.4 (CH_2 , excess of BPP34C10); 70.4 (CH_2); 70.9 (CH_2); 71.2 (CH_2 , excess of BPP34C10); 71.2 (CH_2 , excess of BPP34C10); 114.5 (CH); 116.2 (CH, excess of BPP34C10); 124.1 (CH); 125.2 (CH); 125.5 (CH); 129.1 (CH); 131.6 (CH); 137.2 (C); 137.4 (C); 142.1 (C); 145.8 (CH); 148.8 (C); 151.3 (C); 152.2 (C); 153.0 (CH); 153.3 (CH); 153.9 (C, excess of BPP34C10).

Diffraction-quality crystals of the catenane $4\mathbf{a}(\text{BPP34C10})_2$ were obtained by slow diffusion of ethyl ether into a solution of $3\cdot\text{PF}_6$, $\text{Pd}(\text{en})\text{OTf}_2$ and BPP34C10 in acetonitrile. Anal. Calcd $\text{C}_{104}\text{H}_{120}\text{N}_{10}\text{O}_{20}\text{Pd}_2\cdot 6\text{OTf}\cdot 4\text{CH}_3\text{CN}$: C, 45.52; H, 4.66; N, 6.30. Found C, 45.77; H, 4.42; N, 6.52.

Catenane $4\mathbf{a}(\text{DN38C10})_2\cdot 6\text{PF}_6$. To a solution of $4\mathbf{a},\mathbf{b}\cdot 6\text{PF}_6$ (1.1 mg, 6.0×10^{-4} mmol) in CD_3CN (0.6 mL) was added DN38C10 (1.6 mg, 2.4×10^{-3} mmol). ^1H NMR (500 MHz, CD_3CN) δ : 2.89 (8H, s); 3.06–4.01 (m, excess of DN38C10); 4.35 (8H, br s); 5.53 (br s); 5.77 (4H, m); 5.90 (br s); 6.18 (4H, d, $J = 6.5$ Hz); 6.29 (4H, d, $J = 6.6$ Hz); 6.49 (br s); 6.62 (8H, d, $J = 7.6$ Hz, excess of DN38C10); 7.20 (8H, t, $J = 8.1$ Hz, excess of DN38C10); 7.67 (8H, d, $J = 8.4$ Hz, excess of DN38C10); 7.87 (4H, d, $J = 8.7$ Hz); 7.99 (4H, d, $J = 8.6$ Hz); 8.10 (4H, d, $J = 7.0$ Hz); 8.65 (4H, m); 8.84 (4H, m); 9.04 (4H, d, $J = 7.0$ Hz); ^{13}C NMR (125 MHz, CD_3CN) δ : 47.9 (CH_2); 48.1 (CH_2); 68.4 (CH_2); 69.0 (CH_2 , excess of DN38C10); 70.3 (CH_2 , excess of DN38C10); 70.8 (CH_2); 70.9 (CH_2); 71.4 (CH_2 , excess of DN38C10); 71.4 (CH_2 , excess of DN38C10); 71.5 (CH_2); 71.6 (CH_2); 71.6 (CH_2); 123.4 (CH); 125.1 (CH); 126.3 (CH); 127.3 (CH); 129.3 (CH); 131.9 (CH); 137.2 (C); 141.1 (C); 142.9 (C); 145.9 (C); 151.5 (C); 152.7 (CH); 152.8 (CH); 153.3 (CH); 155.1 (C).

Catenane $5\mathbf{a}(\text{BPP34C10})_2\cdot 6\text{PF}_6$. A solution of $3\cdot\text{PF}_6$ (21.6 mg, 0.046 mmol), $\text{Pt}(\text{en})\text{OTf}_2$ (29.3 mg, 0.053 mmol) in CH_3CN (4.6 mL) and BPP34C10 (123.4 mg, 0.230 mmol) was heated at 55 °C for 8 d. After cooling to room temperature, ethyl ether (100 mL) was added and the precipitate formed was filtered. This solid was suspended in water (30 mL), and Amberlite IRA-402 (0.80 g) was added. The mixture was stirred at room temperature for 24 h. The resin was removed by filtration, and the solvent was evaporated under reduced pressure to give a crude product which was purified by column chromatography (SiO_2 , acetone/ NH_4Cl 1.5M/ MeOH 5:4:1). The product-containing fractions were combined, and the solvents were removed in vacuo. The residue was dissolved in H_2O (30 mL), and an excess of KPF_6 was added until no further precipitation was observed. The solid was filtered and washed with water to yield the catenane (37 mg, 52%) as a yellow solid. Mp = 200–202 °C (decomp). ^1H NMR (500 MHz, CD_3CN) δ : 2.82 (8H, s); 3.16–3.26 (16H, m); 3.55–4.01 (48H, m); 5.02 (4H, br s); 5.12 (4H, br s); 5.23 (16H, br s); 5.68 (4H, s); 7.14 (4H, d, $J = 6.8$ Hz); 7.51 (4H, d, $J = 6.9$ Hz); 7.76 (4H, d, $J = 8.5$ Hz); 7.81 (4H, d, $J = 8.6$ Hz); 7.83 (4H, d, $J = 7.0$ Hz); 8.80 (8H, m); 8.94 (4H, d, $J = 6.9$ Hz); ^{13}C NMR (125 MHz, CD_3CN) δ : 48.6 (CH_2); 49.0 (CH_2); 64.6 (CH_2); 67.7 (CH_2); 69.1 (CH_2); 70.4 (CH_2); 70.9 (CH_2); 71.1 (CH_2); 71.1 (CH_2); 71.1 (CH_2); 115.2 (CH); 125.0 (CH); 125.8 (CH); 126.5 (CH); 129.8 (CH); 132.3 (CH); 137.3 (C); 141.8 (C); 145.1 (C); 146.6 (CH); 148.6 (C); 151.2 (C); 152.2 (C); 154.5 (CH); 154.8 (CH). HRMS-ESI (m/z): Calcd for $[\text{M}-3\text{PF}_6]^{3+}$ 888.5941, found 888.5915; Calcd for $[\text{M}-4\text{PF}_6]^{4+}$ 630.2044, found 630.2015. Anal. Calcd $\text{C}_{104}\text{H}_{132}\text{F}_{36}\text{N}_{10}\text{O}_{20}\text{P}_6\text{Pt}_2$: C, 40.27; H, 4.29; N, 4.52. Found C, 40.05; H, 4.48; N, 4.78.

Catenane $5\mathbf{a}(\text{DN38C10})_2\cdot 6\text{PF}_6$. A solution of $3\cdot\text{PF}_6$ (28.2 mg, 0.060 mmol), $\text{Pt}(\text{en})\text{OTf}_2$ (38.2 mg, 0.069 mmol) in CH_3CN (30 mL), and DN38C10 (76.4 mg, 0.120 mmol) was heated at 55 °C for 8 d. After cooling to room temperature, ethyl ether (500 mL) was added, and the precipitate formed was filtered. A small amount of the solid was recrystallized by slow diffusion of ethyl ether into a acetonitrile solution to give diffraction-quality crystals of the catenane $5\mathbf{a}(\text{DN38C10})_2\cdot 4\text{OTf}\cdot 2\text{PF}_6$. The remaining solid was suspended in water (50 mL), and Amberlite IRA-402 (1.00 g) was added. The mixture was stirred at room temperature for 24 h. The resin was removed by filtration, and the solvent was evaporated under reduced pressure to give a crude product which was purified by column chromatography (SiO_2 , acetone/ NH_4Cl 1.5M/ MeOH 5:4:1). The product-containing fractions were combined and the solvents were removed in vacuo. The residue was dissolved in H_2O (30 mL), and an excess of KPF_6 was added until no further precipitation was observed. The solid was filtered and washed with water to yield the (45 mg, 60%) as a deep red solid. Mp = 205–207 °C (decomp). ^1H NMR (500 MHz, CD_3CN) δ : 2.81 (8H, s); 3.67–4.06 (64H, m); 5.01 (8H, s); 5.55 (br s); 5.83 (m); 5.89 (br s); 6.20 (4H, d, $J = 5.8$ Hz); 6.26 (4H, d, $J = 6.7$ Hz); 7.89 (4H, d, $J = 8.7$ Hz); 8.01 (4H, d, $J = 8.6$ Hz); 8.06 (4H, d, $J = 6.8$ Hz); 8.69 (4H, m); 8.85 (4H, m); 9.04 (4H, d, $J = 6.9$ Hz); ^{13}C NMR (125 MHz, CD_3CN) δ : 48.7 (CH_2); 49.0 (CH_2); 64.4 (CH_2); 68.9 (CH_2); 70.3 (CH_2); 70.8 (CH_2); 71.4 (CH_2); 71.5 (CH_2); 71.6 (CH_2); 71.6 (CH_2); 123.6 (CH); 125.3 (CH); 129.3 (CH); 131.9 (CH); 140.8 (C); 143.0 (C); 145.6 (C); 151.3 (C); 152.1 (C); 153.4 (CH); 153.6 (CH); 154.1 (CH). HRMS-ESI (m/z): Calcd for $[\text{M}-3\text{PF}_6]^{3+}$ 955.2810, found 955.2816; Calcd for $[\text{M}-4\text{PF}_6]^{4+}$ 680.2200, found 680.2202; Calcd for $[\text{M}-5\text{PF}_6]^{5+}$ 515.1831, found 515.1842. Anal. Calcd $\text{C}_{120}\text{H}_{140}\text{F}_{36}\text{N}_{10}\text{O}_{20}\text{P}_6\text{Pt}_2$: C, 43.64; H, 4.27; N, 4.24. Found C, 43.86; H, 4.12; N, 4.10.

1,7-Bis[2-(2-hydroxyethoxy)ethoxy]naphthalene (12b). Compound **12b** was prepared by a modified literature procedure.²² Red

oil (51%). ^1H NMR (300 MHz, CDCl_3) δ : 3.68–3.78 (8H, m); 3.91–4.00 (4H, m); 4.29–4.32 (4H, m); 6.82 (1H, d, $J = 7.3$ Hz); 7.17 – 7.26 (2H, m); 7.39 (1H, d, $J = 8.2$ Hz); 7.63 (1H, d, $J = 2.6$ Hz); 7.71 (1H, d, $J = 8.9$ Hz); ^{13}C NMR (75 MHz, CDCl_3) δ : 61.7 (CH_2); 61.8 (CH_2); 67.4 (CH_2); 68.0 (CH_2); 69.7 (CH_2); 69.8 (CH_2); 72.6 (CH_2); 72.7 (CH_2); 101.7 (CH); 106.0 (CH); 119.2 (CH); 120.5 (CH); 123.4 (CH); 126.6 (C); 129.1 (CH); 130.1 (C); 153.6 (C); 156.5 (C). MS-FAB (3-NBA) (m/z): 336.1 $[\text{M}]^+$. Anal. Calcd $\text{C}_{18}\text{H}_{24}\text{O}_6$: C, 64.27; H, 7.19. Found. C, 64.52; H, 7.05.

Acknowledgment. The authors are indebted to Centro de Computación de Galicia for providing the computer facilities. This research was supported by Xunta de Galicia (PGIDIT06PXIB103224PR), Ministerio de Educación y Cultura and FEDER (CTQ2007-63839/BQU). V.B., D.A.,

and E.P. thank Ministerio de Educación y Ciencia (FPU Program), Xunta de Galicia and Universidade da Coruña for predoctoral fellowships.

Supporting Information Available: Complete ref 20, experimental details for inclusion complexes of **4a**, ^1H NMR, ^{13}C NMR, and 2D experiments for all compounds, crystallographic files (in CIF format) of catenanes **4a**(BPP34C10) $_2$ •6OTf and **5a**(BPP34C10) $_2$ •4OTf•2PF $_6$, and computational details and optimized Cartesian coordinates (BH&H/6-31+G(d) level) for the (MeBIPY $^+$)(DMB) $_2$ and (TPy)(DMB) $_2$ systems. This material is available free of charge via the Internet at <http://pubs.acs.org>.

IC8022425